

Chronic T cell receptor stimulation unmasks NK receptor signaling in peripheral T cell lymphomas via epigenetic reprogramming

Sylvain Carras, ... , Emmanuel Bachy, Laurent Genestier

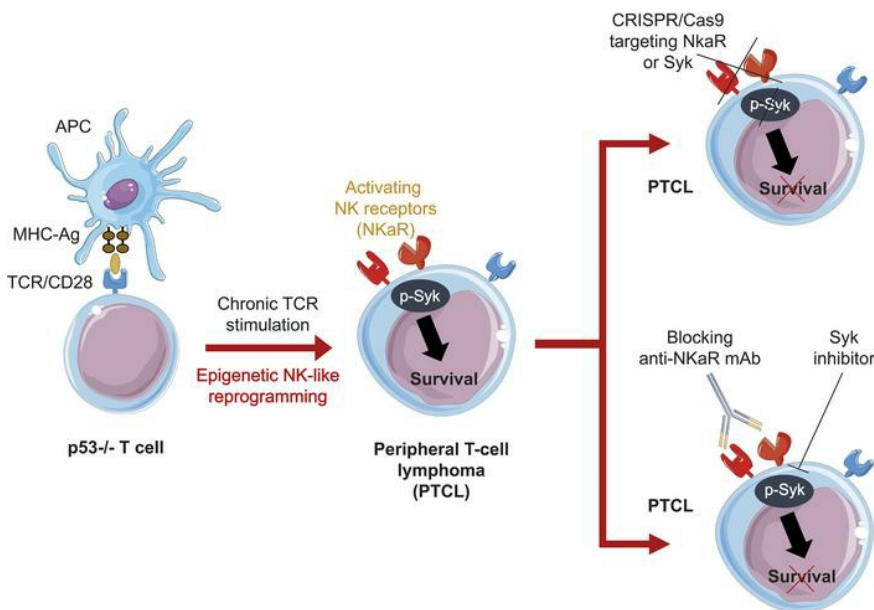
J Clin Invest. 2021;131(13):e139675. <https://doi.org/10.1172/JCI139675>.

Research Article

Hematology

Immunology

Graphical abstract



Find the latest version:

<https://jci.me/139675/pdf>



Chronic T cell receptor stimulation unmasks NK receptor signaling in peripheral T cell lymphomas via epigenetic reprogramming

Sylvain Carras,^{1,2,3} Dimitri Chartoire,^{1,2,3} Sylvain Mareschal,^{1,2,3} Maël Heiblig,^{1,2,3,4} Antoine Marçais,⁵ Rémy Robinot,^{1,2,3} Mirjam Urb,^{1,2,3} Roxane M. Pommier,⁶ Edith Julia,^{1,2,3} Amel Chebel,^{1,2,3} Aurélie Verney,^{1,2,3} Charlotte Bertheau,⁷ Emilie Bardel,^{1,2,3} Caroline Fezelot,^{1,2,3} Lucien Courtois,^{1,2,3} Camille Lours,^{1,2,3} Alyssa Bouska,⁸ Sunandini Sharma,⁸ Christine Lefebvre,^{9,10} Jean-Pierre Rouault,^{1,2,3} David Sibon,¹¹ Anthony Ferrari,⁶ Javeed Iqbal,⁸ Laurence de Leval,¹² Philippe Gaulard,^{13,14} Alexandra Traverse-Glehen,^{1,2,3,7} Pierre Sujobert,^{1,2,3,15} Mathieu Blery,¹⁶ Gilles Salles,^{1,2,3,4} Thierry Walzer,⁵ Emmanuel Bachy,^{1,2,3,4} and Laurent Genestier^{1,2,3}

¹UR LIB, Faculté de Médecine Lyon Sud, Université Claude Bernard Lyon I, Lyon, France. ²Hospices Civils de Lyon, Lyon, France. ³Centre de Recherche en Cancérologie de Lyon – Equipe Labellisée La Ligue 2017, INSERM U1052, Centre National de Recherche Scientifique (CNRS) UMR 5286, Université de Lyon, Centre Léon Bérard, Lyon, France. ⁴Department of Hematology, Hospices Civils de Lyon, Lyon, France. ⁵INSERM U1111, CNRS UMR 5308, Centre International de Recherche en Infectiologie, Lyon, France. ⁶Synergie Lyon Cancer, Plateforme de Bioinformatique “Gilles Thomas” Centre Léon Bérard, Lyon, France. ⁷Department of Pathology, Hospices Civils de Lyon, Lyon, France. ⁸Department of Pathology and Microbiology, University of Nebraska Medical Center, Omaha, Nebraska, USA. ⁹Department of Genetics of Hematological Malignancies, Grenoble University Hospital, Grenoble, France. ¹⁰INSERM U1209, CNRS UMR 5309, Grenoble Alpes University, Institute for Advanced Biosciences, Grenoble, France. ¹¹Institut Imagine, INSERM U1163, CNRS ERL 8254, Université Paris Descartes, Sorbonne Paris-Cité, Laboratoire d'Excellence GR-Ex, Paris, France. ¹²Institute of Pathology, Centre Hospitalier Universitaire Vaudois (CHUV), Université de Lausanne, Lausanne, Switzerland. ¹³INSERM U955, Université Paris-Est, Créteil, France. ¹⁴Department of Pathology, Assistance Publique–Hôpitaux de Paris (AP-HP), Groupe Hospitalier Henri-Mondor, Créteil, France. ¹⁵Laboratory of Hematology, Centre Hospitalier Lyon Sud, Hospices Civils de Lyon, Pierre-Bénite, France. ¹⁶Innate Pharma, Marseille, France.

Peripheral T cell lymphomas (PTCLs) represent a significant unmet medical need with dismal clinical outcomes. The T cell receptor (TCR) is emerging as a key driver of T lymphocyte transformation. However, the role of chronic TCR activation in lymphomagenesis and in lymphoma cell survival is still poorly understood. Using a mouse model, we report that chronic TCR stimulation drove T cell lymphomagenesis, whereas TCR signaling did not contribute to PTCL survival. The combination of kinome, transcriptome, and epigenome analyses of mouse PTCLs revealed a NK cell–like reprogramming of PTCL cells with expression of NK receptors (NKR) and downstream signaling molecules such as Tyrobp and SYK. Activating NKR were functional in PTCLs and dependent on SYK activity. In vivo blockade of NKR signaling prolonged mouse survival, demonstrating the addiction of PTCLs to NKR and downstream SYK/mTOR activity for their survival. We studied a large collection of human primary samples and identified several PTCLs recapitulating the phenotype described in this model by their expression of SYK and the NKR, suggesting a similar mechanism of lymphomagenesis and establishing a rationale for clinical studies targeting such molecules.

Introduction

Peripheral T cell lymphomas (PTCLs) are highly heterogeneous, comprising at least 30 post-thymic (i.e., mature) T or NK cell-derived entities according to the current 2016 WHO classification (1). PTCLs represent approximately 5%–10% of all non-Hodgkin lymphomas (NHLs) in Western countries, and the incidence is even higher in Asia and Central and South America (2). Aside from cutaneous mycosis fungoides (MF) and Sézary syndrome (SS), angioimmunoblastic T cell lymphoma (AITL) and PTCL–not otherwise specified (PTCL–NOS) are the most prevalent diseases. Compared with their B cell counterpart, most PTCLs have a poor prognosis,

with a 5-year overall survival rate barely exceeding 30%, and chemotherapy regimens that cure many patients with B cell NHL have thus far been relatively ineffective against PTCLs, emphasizing the need for innovative approaches (2).

T cell receptor (TCR) signaling is the major growth-regulatory machinery of normal T cells. Evidence supporting its important role in the biology of various PTCL entities has recently been published. A specific translocation (t[5;9] [q33;q22]) in some PTCLs that leads to the generation of an abnormal ITK-SYK fusion protein, constitutive tyrosine kinase activity, and the development of PTCLs been reported in a mouse model (3). Recurrent activating mutations in TCR and costimulatory receptor pathway genes such as *RHOA*, *FYN*, *LCK*, *PRKCQ*, *PLCG1*, *VAV1*, *CD28*, and *CARD11* have been described in several PTCL entities such as cutaneous T cell lymphomas (CTCLs) (4–6), adult T cell leukemia/lymphoma (ATLL) (7), AITL, and PTCL–NOS (8–12). Aside from the ITK/SYK translocation and the *RHOA*

Conflict of interest: MB is a former employee of Innate Pharma.

Copyright: © 2021, American Society for Clinical Investigation.

Submitted: May 1, 2020; **Accepted:** May 24, 2021; **Published:** May 27, 2021.

Reference information: *J Clin Invest.* 2021;131(13):e139675.

<https://doi.org/10.1172/JCI139675>.

G17V mutation (13, 14), the role of these genomic alterations in PTCL biology remains elusive, as they may constitute acquired secondary events. In the past years, chronic TCR stimulation has been suspected in the lymphomagenesis of some PTCLs (15). For instance, enteropathy-associated T cell lymphoma (EATL) is a well-recognized complication of celiac disease that is thought to be linked to chronic antigenic stimulation (16). However, recent work highlighted the finding that neoplastic cells are not specific to gliadin, the main antigen responsible for celiac disease, and may be transformed through chronic bystander activation (17). T cell large granular lymphocytic leukemia (T-LGL), SS, hepatosplenic T cell lymphoma (HSTL), and breast implant-associated anaplastic large cell lymphoma (ALCL) also seem to occur in a setting of sustained immune stimulation (18–21), although direct evidence of a driving role of chronic TCR stimulation is lacking. Finally, conventional T cell lymphomagenesis has been demonstrated to be dependent on TCR signaling in murine models, such as in *Snf5* conditionally inactivated T cells (22), while exposure to chronic bacterial antigens drives lymphomagenesis of unconventional NKT cells in *p53*^{-/-} mice (23, 24).

Collectively, these clinical and experimental data point toward a central role for TCR signaling in PTCL, although a direct link between chronic TCR stimulation and conventional T cell lymphomagenesis has not been formally established. In this study, we attempted to unravel the mechanisms of T cell lymphoma development in the context of chronic TCR stimulation using conventional *p53*^{-/-} T cells, since *TP53* mutations or copy number alterations have been recurrently described in several PTCL entities (4, 6, 25–27).

Results

Chronic TCR stimulation drives *p53*^{-/-} T cell lymphomagenesis. To mimic chronic TCR stimulation, we took advantage of T cell homeostatic proliferation or lymphopenia-induced proliferation (LIP) (28), which is driven by cytokines and chronic TCR signaling generated by self-MHC-TCR interactions. To this end, purified mature T cells from WT or *p53*^{-/-} mice were transferred into *CD3ε*^{-/-} recipient mice (which lack mature T cells). In this condition, transferred WT or *p53*^{-/-} T lymphocytes rapidly proliferated in the spleen and lymph nodes (LNs) (Supplemental Figure 1A; supplemental material available online with this article; <https://doi.org/10.1172/JCI139675DS1>), acquired activated and memory phenotypes (Supplemental Figure 1B), and expanded in *CD3ε*^{-/-} recipient mice (Supplemental Figure 1C). Whereas 75% of *CD3ε*^{-/-} recipient mice receiving WT T lymphocytes (hereafter referred to as WT>*CD3ε*KO mice) were still alive 450 days after transfer, all mice transferred with *p53*^{-/-} T lymphocytes (hereafter referred to as *p53*KO>*CD3ε*KO mice) had died within 343 days (median survival = 224 days; Figure 1A). As a control, we also transferred *p53*^{-/-} T lymphocytes into WT recipient mice (hereafter referred to as *p53*KO>WT mice), which triggered neither homeostatic proliferation (Supplemental Figure 1D) nor death even 450 days after transfer (Figure 1A). Sixty percent of the *p53*KO>*CD3ε*KO mice exhibited adenomegalies, splenomegaly, and hepatomegaly (Figure 1B and Supplemental Figure 2A) associated with a complete effacement of the normal LN, spleen, and liver architecture (Figure 1C), as well as massive

expansion of large T lymphocytes (*CD3*⁺*Thy1*⁺*CD19*⁻) (Supplemental Table 1 and Supplemental Figure 2B). High-throughput sequencing of the TCR repertoire showed monoclonal expansion of T lymphocytes in all lymphoproliferations tested (Figure 1D and Supplemental Table 2). Altogether, the results obtained in the *p53*KO>*CD3ε*KO mice defined these monoclonal T lymphocyte expansions as PTCLs, in contrast to the WT>*CD3ε*KO mice that did not develop PTCL (Figure 1B). To confirm the neoplastic nature of these proliferations, we transferred total cells from enlarged spleens or livers into WT C57BL/6 recipient mice. These recipient mice developed all the characteristics of the donor mice, with rapid enlargement of LNs, splenomegaly, and hepatomegaly requiring euthanasia (Supplemental Figure 2C).

Murine PTCLs (mPTCLs) downregulated T cell markers such as TCRβ and CD5, did not express TCRγδ, were not CD1d restricted, and were mostly CD8⁺ (Supplemental Figure 2, D and E). They were also CD62L^{lo}CD44⁺CD122⁺CD25⁻CD127⁻, defining an effector memory phenotype (Figure 1E and Supplemental Figure 2E). Activation markers such as CD54 and B220 were significantly upregulated in all mPTCLs compared with expression in normal T cells (Figure 1E), whereas PD1 and LAG3 were only expressed in 40% of mPTCL cells (Supplemental Figure 2E). Finally, the death receptor Fas/CD95, which is highly expressed in activated T cells, was strongly downregulated in mPTCL cells (Supplemental Figure 2F).

TCR and IL-15 are not required for mPTCL survival. To confirm the involvement of chronic TCR stimulation in mPTCL development, we studied the gene expression profile (GEP) of these mPTCLs in comparison with normal resting and activated T cells. Previous reports established that gene expression of CD247 (*CD3ζ*), LCK, and LAT was downregulated upon repeated stimulation arising in the context of chronic infection or autoimmunity (29). We thus focused on the TCR signaling pathway using gene set enrichment analysis (GSEA), as previously described in NKT lymphomas (23). The expression of genes involved in the TCR signaling pathway, in particular CD247 (*CD3ζ*), LCK, and LAT, was markedly downregulated compared with expression in normal T cells (*P* = 0.007) (Figure 2, A and B), supporting the role of chronic TCR stimulation in this model of lymphomagenesis.

To further investigate the role of TCR signaling in these mPTCLs and, more specifically, to ascertain whether constitutive TCR signaling is required for mPTCL survival, we used cyclosporine A (CsA), a calcineurin inhibitor known to strongly suppress TCR signaling. Although in vivo administration of CsA has already been shown to inhibit PTCL survival in a TCR signaling-dependent manner (22, 23), it did not prolong the survival of C57BL/6 mice transferred with PTCL cells from our model, suggesting that mPTCL survival did not rely on constitutive TCR activation (Figure 2C). To further test this point, mPTCL cells were genetically invalidated for the TCR/CD3 signaling complex using sgRNA/Cas9 ribonucleoprotein (RNP) targeting the *Cd3ε* gene to achieve a protein knockdown of CD3ε at rates of more than 85% (Supplemental Figure 3A). Mice transferred with *Cd3ε*-invalidated mPTCL cells did not survive longer than those transferred with mPTCL cells transfected with control sgRNA/Cas9 RNP (Figure 2D), confirming that constitutive TCR signaling was not required for mPTCL survival.

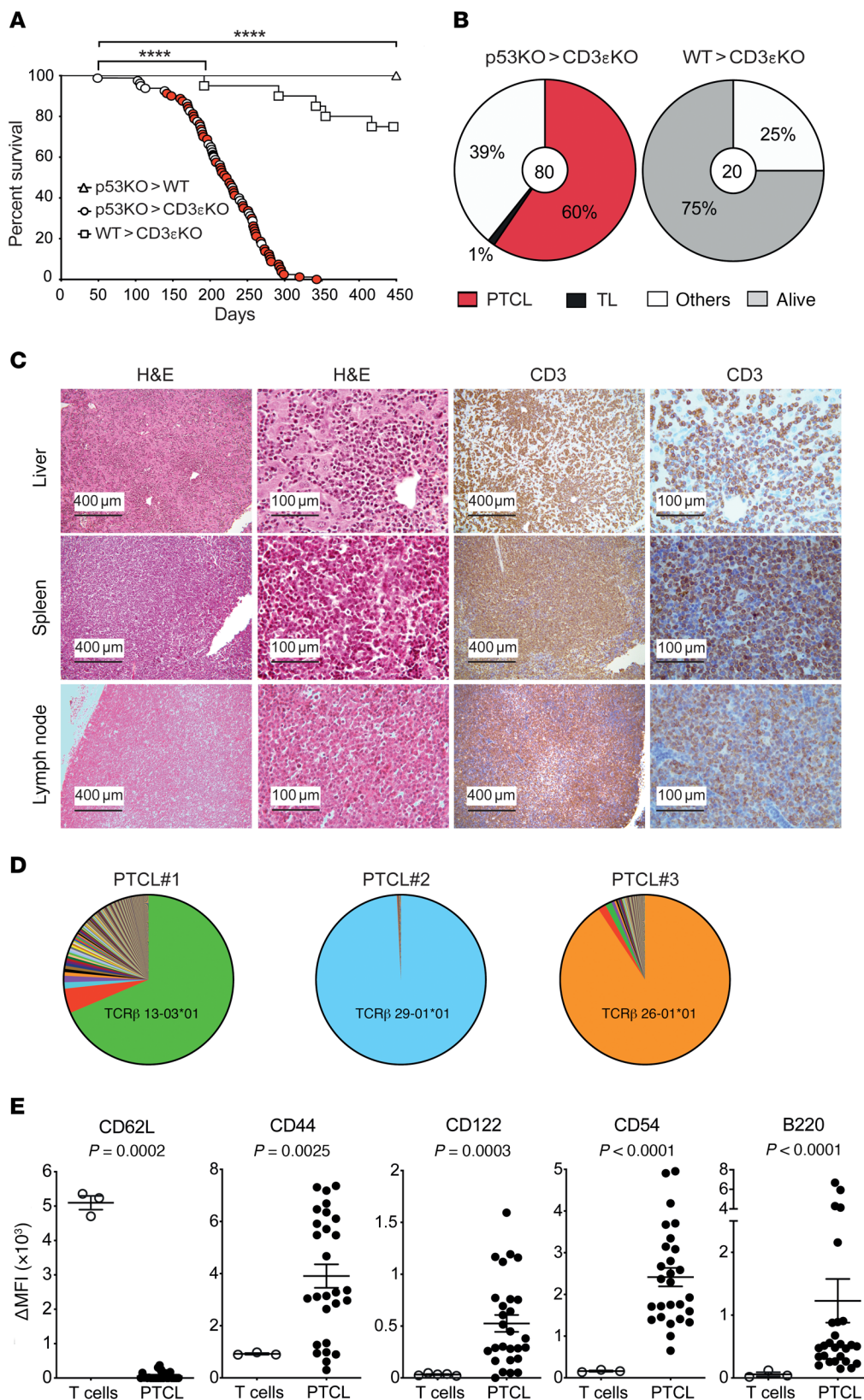


Figure 1. Chronic TCR stimulation promotes T cell lymphomagenesis. (A) Kaplan-Meier survival curves for CD3 $\epsilon^{-/-}$ mice receiving WT cells (WT>CD3 ϵ KO, squares, $n = 20$) or p53 $^{-/-}$ T cells (p53KO>CD3 ϵ KO, circles, $n = 80$) and for WT (C57BL6 CD451.1) mice receiving p53 $^{-/-}$ T cells (CD451.2) (p53KO>WT, triangle, $n = 11$). In the WT>CD3 ϵ KO group, recipient mice alive on day 450 were sacrificed and evaluated. For the p53KO>WT group, all mice were still alive 450 days after transfer. **** $P < 0.0001$, by log-rank test and Holm's post hoc correction. For the p53KO>CD3 ϵ KO group, the circles are colored according to the mouse's cause of death: data points for mice that died of PTCL are shown in red, thymic lymphomas (TL) in black, and others (no lymphoma) in white. (B) Spectrum of causes of death for p53KO>CD3 ϵ KO or WT>CD3 ϵ KO mice. Mice alive on day 450 were categorized as "alive" and were then sacrificed. (C) Representative histological micrographs of formalin-fixed, H&E- or anti-CD3-stained liver, spleen, and LNs obtained from a mPTCL. Scale bars: 100 μ m; 400 μ m. (D) Pie chart representation of TCR β clonality in 3 representative mPTCL samples among 16 tested. (E) Surface expression of CD62L, CD44, CD122, CD54, and B220 measured by flow cytometry (Δ MFI) in mPTCL cells ($n = 26$) compared with normal T cells ($n = 3$). P values were determined by Mann-Whitney U test comparing mPTCL cells with control T cells.

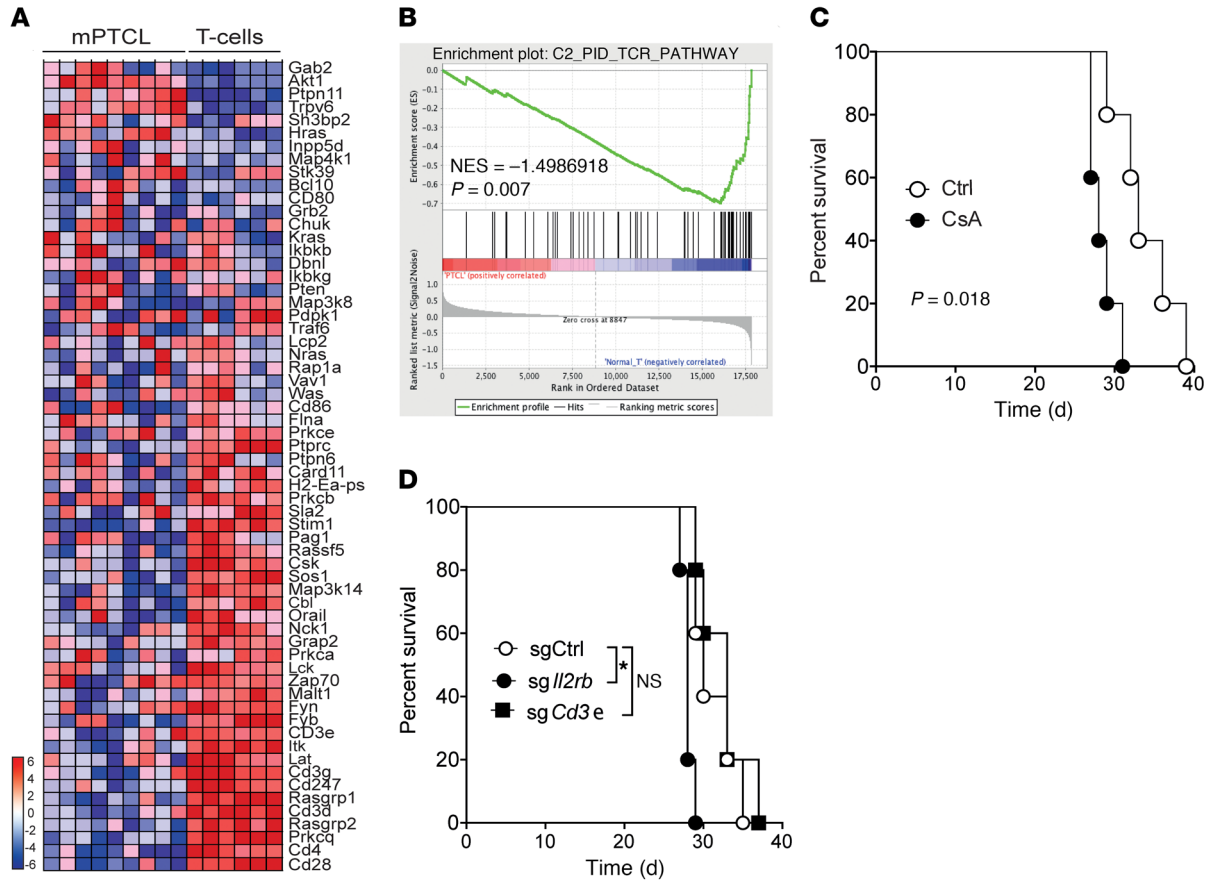


Figure 2. TCR stimulation is required for lymphomagenesis but dispensable for mPTCL survival. (A) Heatmap of all genes included in the GSEA for the TCR signaling pathway in mPTCL cells compared with normal resting and activated T cells. (B) GSEA of a set of genes from the TCR signaling pathway. The downward deflection indicates enrichment of the TCR signaling pathway signature in normal T cells ($P = 0.007$, nominal permutation P value based on 1000 permutations). NES, normalized enrichment score. (C) Kaplan-Meier survival curves for WT mice receiving mPTCL cells and treated with CsA (20 mg/kg; $n = 5$) or vehicle alone (Ctrl; $n = 5$). P value was determined by log-rank test. Shown are results from 1 representative experiment among 3 tested with different PTCLs. (D) Kaplan-Meier survival curves for WT mice ($n = 5$ for each group) transferred with mPTCL cells genetically invalidated for *Cd3e* or *Il2rb* using Alt-R CRISPR/Cas9 sgRNA targeting either of these genes, or transfected with control sgRNA (sgCtrl). $*P < 0.05$, by log-rank test and Holm's post hoc correction. Data are representative of 2 independent experiments using different mPTCL cells.

We next analyzed whether deliberate TCR activation of mPTCL cells may affect survival of these mice in vivo. Injection of an agonist anti-CD3 mAb did not modify the survival of most *CD3e*^{-/-} recipient mice transferred with PTCL cells (Supplemental Figure 3B), suggesting that the TCR was not involved in mPTCL survival in vivo.

Having excluded TCR signaling as the major prosurvival pathway in mPTCLs, we then speculated that cytokines known to be crucial for T cell proliferation and/or survival may be implicated. Among the cytokines involved in T cell homeostatic proliferation, IL-15 plays a central role. Since the IL-15R β chain CD122 was highly upregulated in mPTCLs (Figure 1E) and IL-15 was described as a proinflammatory cytokine responsible for genomic instability and T cell lymphoma/leukemia development (30–32), we investigated whether IL-15 was involved in mPTCL survival in our model. As a first approach, we transferred mPTCL cells into WT or *IL-15*^{-/-} syngeneic mice and observed no difference in mPTCL development, since both groups of mice had similar survival curves (Supplemental Figure 3C). Keeping in mind the possible autocrine IL-15/IL-15R loop described in CD8⁺ T cell lymphoma/leukemia devel-

opment (30, 32), we also tested the effect of genetic invalidation of CD122 or an anti-CD122-blocking antibody on mPTCL survival. Transfer of mPTCL with pharmacological or genetic invalidation of CD122 did not increase the survival of C57BL/6 recipient mice (Figure 2D and Supplemental Figure 3, A and D), demonstrating that IL-15 was not required for mPTCL survival in vivo. To rule out other cytokines involved in T cell survival, we treated WT syngeneic recipient mice transferred with mPTCLs with inhibitors of JAK1/2 (ruxolitinib) or JAK1/3 (tofacitinib), which participate in IL-2R, IL-4R, IL-7R, and IL-15R signaling. Neither inhibitor had an effect on mPTCL survival (Supplemental Figure 3E).

Ectopic expression and activation of SYK in murine and human PTCLs. To identify molecular mechanisms involved in mPTCL survival, we first used a kinase array assay to evaluate the constitutively activated tyrosine kinases in mPTCLs compared with normal T cells. Among the 144 peptides present on the array, 43 and 37 peptides associated with SYK and Zap70 activity, respectively, were phosphorylated in the mPTCL lysates (Figure 3A). Kinases upstream of SYK or ZAP70, such as BLK, LCK, and FYN, were also constitutively activated in mPTCLs (Figure 3A). Since

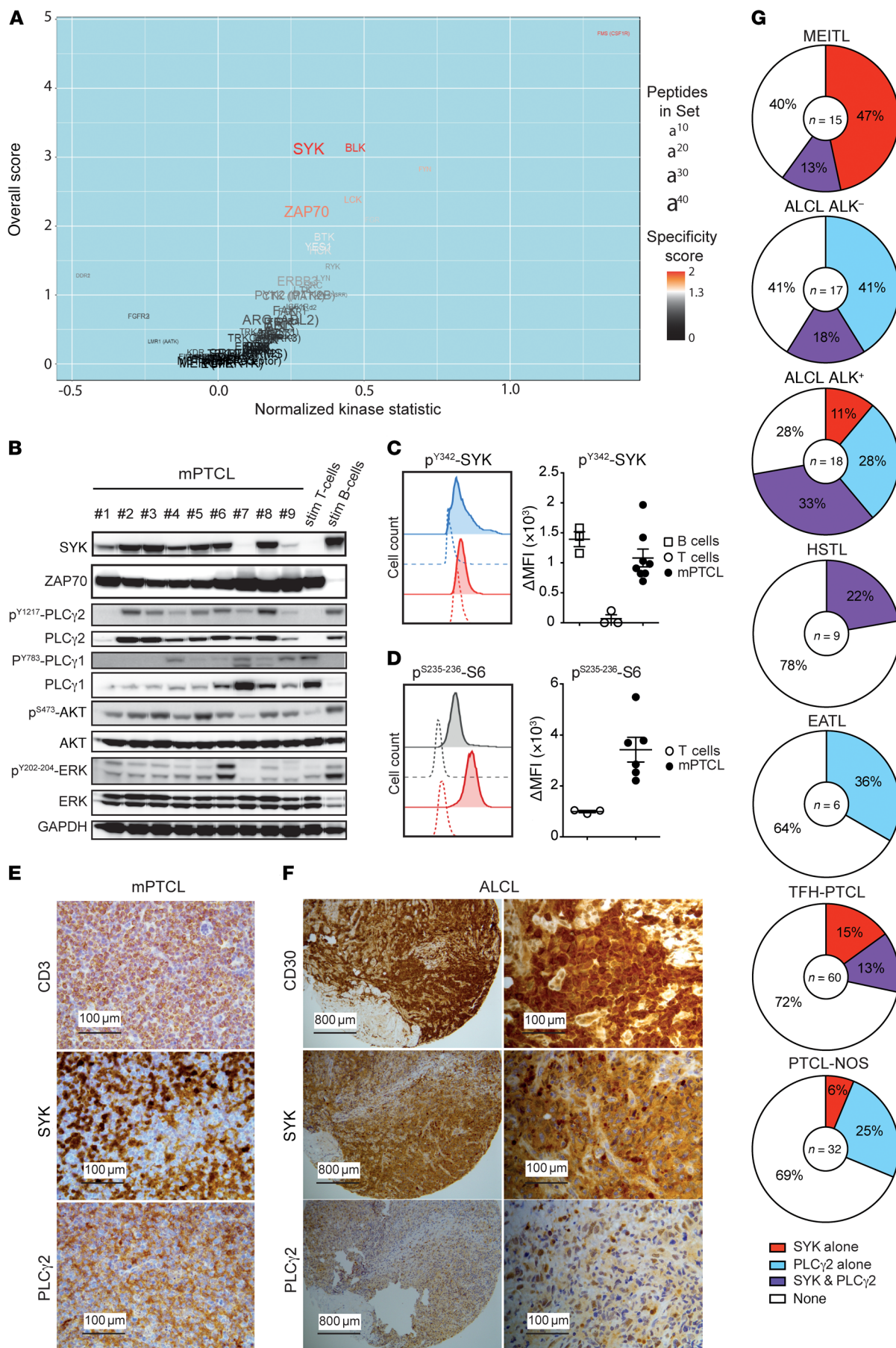


Figure 3. SYK and downstream signaling pathways are constitutively activated in mPTCLs. (A) Volcano plot representation of the PamGene GeneGO analysis of tyrosine kinase activation in mPTCL cells ($n = 18$) compared with normal T cells ($n = 3$). The peptide contribution to upstream kinases was determined. (B) Western blots show the expression of SYK and ZAP70, as well as the expression and activation of PLC γ 1, PLC γ 2, AKT, and ERK in mPTCL cells compared with purified and stimulated (stim) normal B and T cells from WT mice, used as positive control. GAPDH was used as a loading control. (C) Representative FACS analysis of SYK tyrosine phosphorylation (p^{Y342}-SYK) in mPTCL cells (red) in the basal state (red solid line) and after SYK pharmacological inhibition with P505-15 (red dashed line), as well as in control B cells (blue) in the basal state (blue dashed line) and after B cell receptor (BCR) stimulation (blue solid line), as measured by flow cytometry. Associated scatter plot shows SYK tyrosine phosphorylation expressed as the Δ MFI between basal and P505-15-treated mPTCL cells ($n = 8$) compared with the Δ MFI between basal and BCR-stimulated B cells ($n = 3$), or between basal and TCR-stimulated T cells ($n = 3$). (D) Representative FACS analysis of p^{S235-236}-S6 in mPTCL cells (red) or control T cells (gray) in the basal state (solid lines), as well as after mTORC1 pharmacological inhibition with rapamycin (dash lines). Associated scatter plot shows the Δ MFI between basal and rapamycin-treated conditions in mPTCL cells ($n = 6$) compared with T cells ($n = 3$). (E) Immunohistochemical staining for CD3, SYK, and PLC γ 2 in representative mPTCL cells (liver). Scale bars: 100 μ m. (F) Immunohistochemical staining for CD30, SYK, and PLC γ 2 in representative human ALK⁺ ALCL. (G) SYK and PLC γ 2 expression in lymphoma cells from 7 different entities of human PTCLs. The TFH-PTCLs include AITL and PTCL-NOS with TFH-like features according to the 2016 WHO classification.

SYK was not expressed in normal mature T cells (Figure 3B), we first examined the presence of SYK in enriched mPTCL cells (purity >96%) by Western blotting and IHC. SYK was expressed in 8 of 9 and 4 of 5 mPTCLs tested, respectively (Figure 3, B and E, and see complete unedited blots in the supplemental material). We also confirmed the constitutive activation of SYK in mPTCLs compared with normal activated B and T cells using phospho-flow analyses (Figure 3C). We then studied the expression and constitutive activation of classical downstream effectors of the SYK signaling pathway, such as PLC γ 1, PLC γ 2, AKT, ERK, and S6 kinase. Surprisingly, we found that PLC γ 2, which is generally not expressed in normal T cells (Figure 3B), was also expressed and constitutively activated in almost all mPTCLs tested (Figure 3, B and E). In contrast, the expression of PLC γ 1, the most common PLC γ isoform in normal T cells (Figure 3B), was decreased in 7 of 9 mPTCLs tested and showed only minor activation. Downstream kinases such as AKT, ERK, and S6 were also constitutively activated in all mPTCLs tested (Figure 3, B and D). Next, we performed immunohistochemical analyses to assess the expression of SYK and PLC γ 2 in a cohort of 157 primary human PTCLs representing 7 different entities (Supplemental Table 3). We found that SYK was expressed in 60% of monomorphic epitheliotropic intestinal T cell lymphoma (MEITL) cells and 44% of anaplastic lymphoma kinase-positive (ALK⁺) ALCL cells (Figure 3F), as well as approximately 30% of T follicular helper PTCL (TFH-PTCL) cells, 20% of ALK⁻ ALCL and HSTL cells, and 10% of PTCL-NOS cells. PLC γ 2 was mostly coexpressed with SYK, with the exception of some ALCL (41%), PTCL-NOS (25%), and EATL cells, which only expressed PLC γ 2 (Figure 3G). Taken together, these results highlight the expression of SYK and its downstream effectors in both mPTCLs and a subset of human PTCL.

mPTCLs have a NK-like GEP. To define potential receptors upstream of the SYK and PLC γ 2 signaling pathway, we compared the GEP of 9 mPTCLs with normal resting and activated T cells. The top downregulated and upregulated genes (log₂ fold change [FC] >1; adjusted $P < 0.05$) between mPTCLs and normal T cells are depicted in the heatmap and volcano plot (Supplemental Figure 4A and Figure 4A). We found that *Syk* and *Plcg2* were among the upregulated genes, confirming our previous results from kinome and Western blot studies. Surprisingly, many genes associated with T cell differentiation or T cell identity, such as *Cd4*, *Cd8*, *Cd5*, *Cd28*, *Thy1*, and *Bcl11b*, were downregulated in mPTCLs, whereas genes associated with cytotoxicity and the NK cell lineage, such as *Tyrbp* (DAP12), *Fcer1g*, *Ncr1* (NKp46), *Cd244* (2B4), and *Gzma*, were upregulated in comparison with expression levels in normal T cells (Figure 4A). To further refine the similarities between mPTCL and a potential normal cell subtype counterpart, we also compared these GEPs with a wide array of immunological cell populations ranging from immature T cells to NK and NKT cell subsets from the Immunological Genome Project (ImmGen) mouse gene atlas and from our own previous cohort (23). Interestingly, hierarchical clustering based on the 1% most variably expressed genes revealed that most mPTCLs (5 of 9) clustered with NK cells, whereas the others clustered with immature T cell populations, mainly NKT and $\gamma\delta$ T cells (Figure 4B). Clustering was driven by 3 gene sets. The first one was highly enriched in “cancer proliferation” genes mostly expressed in mPTCL, NK cells, as well as in immature T cell populations. The second gene set was highly expressed in most mPTCLs, NK cells, NKT cells, as well as in effector and memory CD8⁺ T cells and associated with “antigen response” and “NK cell” signatures. The third gene set was negative in mPTCLs and included several T cell genes (Figure 4C and Supplemental Table 4). When focusing on differential gene expression between NK cells versus T cells (y axis) and mPTCLs versus T cells (x axis), most genes were comparably regulated in NK cells and mPTCLs (as evidenced on the diagonal of the figure), confirming the similarity between NK cells and mPTCLs (Figure 4D). When we investigated the genes upregulated in NK cells and mPTCLs (top-right quadrant), we found that many genes were associated with cytotoxicity, the NK cell receptor (NKR), and signaling of NK cell-activating receptors (NKARs), suggesting a reprogramming of chronically stimulated T lymphocytes into NK-like PTCLs expressing several features of NK cells. Deletion of *Bcl11b* in mature T cells is known to result in reprogramming of T cells toward NK-like cells (33), demonstrating that *Bcl11b* is not only necessary for T cell development but also required to restrict mature T cell access to NK cell programs. We confirmed at the protein level the profound downregulation of *Bcl11b* in mPTCLs compared with expression in normal T cells (Supplemental Figure 4B), suggesting that this downregulation may be a driver of NK cell-like reprogramming of mPTCL cells.

Murine PTCLs exhibit an epigenetic NK cell-like reprogramming. We next addressed whether NK cell-like reprogramming of mPTCL could be the consequence of chromatin remodeling using an assay for transposase-accessible chromatin with high-throughput sequencing (ATAC-Seq). Applying the same analytic strategy of comparing mPTCL with immature and mature T cell populations as well as mature NK cells (from ImmGen and from our own

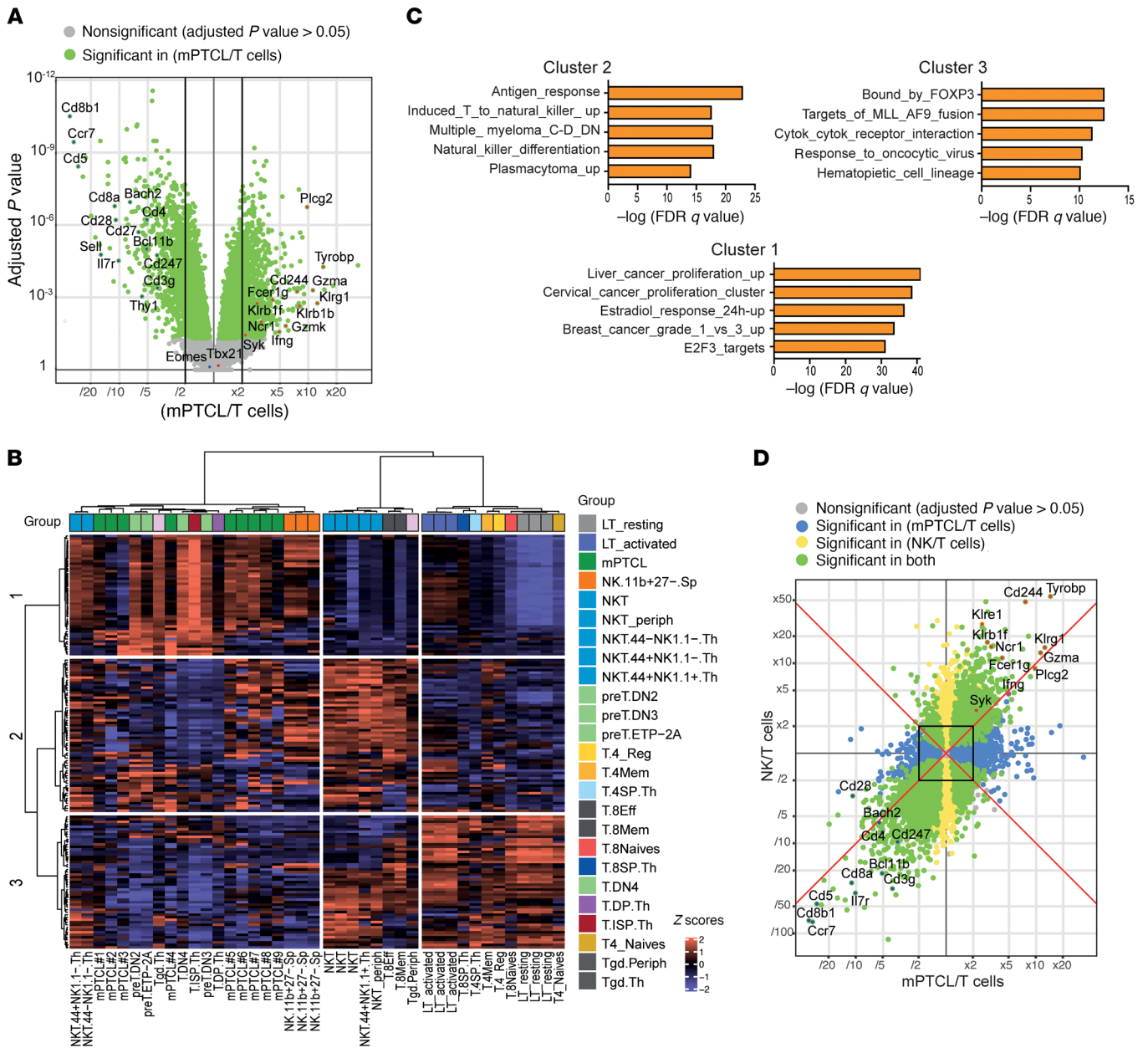


Figure 4. Murine PTCLs downregulate T cell genes and express a NK-like transcriptome. (A) Volcano plot of genes differentially expressed between mPTCL cells ($n = 9$) and normal T cells ($n = 6$). The vertical black lines delimit the 2-FC effects. Upregulated genes in mPTCL cells compared with normal T cells are located on the right and downregulated genes on the left. Informative upregulated genes have been color-coded in red and the downregulated in blue. **(B)** Unsupervised clustering (using the Euclidean distance, Ward agglomeration method) based on the 1% of genes most variably expressed between immature and mature T cell populations as well as mature NK cells (data are from ImmGen and our own cohort). This clustering analysis generated 3 gene clusters (1, 2, and 3), defined on the left of the panel. **(C)** Representation of the 5 most highly significant C2 (Molecular Signatures Database [MSigDB]) gene set names of the 3 different gene clusters defined in **B**. **(D)** Comparison of genes differentially expressed between normal NK and T cells (y axis) and mPTCLs and normal T cells (x axis). Yellow dots correspond to genes differentially expressed, at a multiple-testing, adjusted P value of 0.05, between NK and T cells; blue dots correspond to genes differentially expressed between mPTCLs and T cells; and green dots represent genes differentially expressed in both conditions. The names of some of the most informative genes are indicated in the upper-right and lower-left quadrants.

cohort) to analyze the chromatin landscape, we identified 98,375 high-quality open chromatin regions (OCRs). Hierarchical clustering or PCA analyses on all these peaks revealed (a) the global epigenetic proximity between mPTCLs and NK cells and, to a lesser extent, mature NKT and effector/memory CD8⁺ T cells, and (b) the more distant relation between mPTCL and immature T cell subsets (Figure 5A and Supplemental Figure 4C). This reinforces previous

transcriptional data and demonstrates that mPTCL cells underwent an epigenetic reprogramming toward NK cells. Supervised analysis further supported this chromatin remodeling of mPTCL cells toward NK cells. Compared with T cells from our own cohort, mPTCL cells showed greater accessibility to 3025 OCRs (FDR < 0.01) mostly associated with NK signatures from the ImmGen mouse gene atlas (FDR < 10⁻⁴⁵) and lower accessibility to 4526

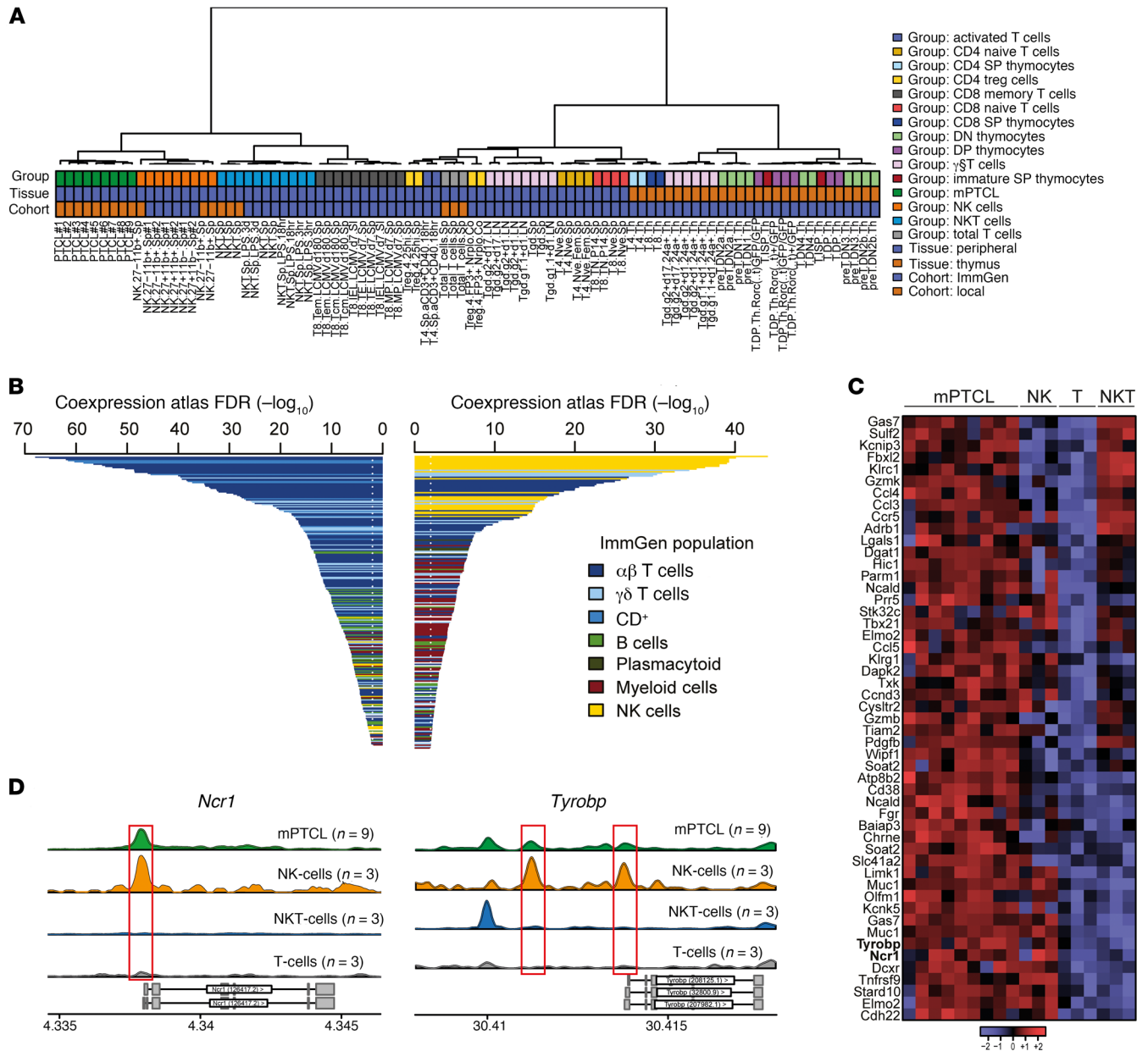


Figure 5. Epigenetic reprogramming of mPTCLs into NK-like cells. (A) Unsupervised clustering (Euclidean distance, Ward agglomeration method) of mPTCL cells, immature and mature T cell populations, as well as mature NK cells from ImmGen and from our own cohort, based on the normalized accessibility of all 98,375 OCRs identified in ATAC-Seq. **(B)** Each bar represents a gene expression-based signature of a specific mouse cell population in the ImmGen atlas, colored according to broader population classes. Bar lengths (x axis) indicate the statistical significance of the overlap between genes in the signature and genes with differential chromatin accessibility in ATAC-Seq between mPTCL cells and normal T cells (ToppFun coexpression test FDR < 0.01). Cell populations whose representative genes harbor OCRs more accessible in normal T cells and mPTCL cells are presented respectively in the left and right panels. **(C)** Heatmap of chromatin accessibility in the 51 OCRs located in the promoter regions of genes involved in NK signatures presented in Figure 4E. **(D)** ATAC-Seq tracks from normal T cells, NKT cells, and NK cells, as well as mPTCL cells around *Tyrobp* and *Ncr1* (average TMM-normalized CPMs per group in 50 bp wide bins). OCRs surrounded in red are significantly different (FDR < 5%) between conditions (mPTCL ≠ T and NKT; NK ≠ T and NKT).

OCRs (FDR < 0.01) mostly associated with ImmGen $\alpha\beta$ T cell signatures (FDR < 10^{-68}) (Figure 5B). Further analysis of OCRs in the promoter regions involved in these NK signatures unveiled several genes, such as *Gas7*, *Klrc1*, *Gzmk*, *Gzmb*, *Tyrobp*, and *Ncr1* (Figure 5C). For instance, *Tyrobp* and *Ncr1*, which are highly expressed in mPTCLs compared with expression levels in normal T cells and NKT cells, exhibited greater OCR heights in mPTCL and NK cell versus T cell and NKT cell promoter regions (Figure 5D).

To confirm these epigenetic changes, we also performed genome-wide DNA methylation analysis using reduced representation bisulfite sequencing (RRBS) on T cells, NK cells, and mPTCL cells. PCA revealed that mPTCL cells clustered between T cells and NK cells (Supplemental Figure 4D). To compare these results with ATAC-Seq, we calculated for each sample the average methylation across ATAC-Seq peaks with a positive FC (FDR < 0.01, logFC > 0, $n = 144$) and those with a negative FC (FDR < 0.01, log-

FC <0, $n = 239$). The box plots in Supplemental Figure 4E show that the methylation profile of mPTCL cells was closer to that of NK cells for both peak sets.

Mature NK cell development is driven by transcription factors such as T-bet and Eomes (34). We therefore studied the expression of these 2 transcription factors in mPTCL cells compared with normal T and NK cells. Whereas T-bet and Eomes were not upregulated at the mRNA level in mPTCL cells compared with normal T cells (Figure 4A), they were both significantly overexpressed at the protein level in mPTCL cells (Supplemental Figure 4F). This suggests that post-transcriptional regulation, in addition to epigenetic modifications, is coordinated to induce NK-like reprogramming of mPTCL cells.

Activating and inhibitory NKR are expressed in murine and human PTCLs. To further study NK-like reprogramming of mPTCL cells during chronic TCR stimulation, we analyzed NKR expression on 23 mPTCL cells using multiparametric flow cytometry to evaluate the expression of 6 NKaRs and 6 NK cell inhibitory receptors (NKiRs). Our data showed the expression of at least 1 NKR on 96% (22 of 23) of mPTCL cells and at least 1 NKaR or NKiR on 66% (15 of 23) and 70% (16 of 23) of mPTCL cells, respectively (Supplemental Figure 5A). Among the NKaRs, NK1.1, NKG2D, 2B4, and CD16-32 were significantly expressed in most mPTCL cells compared with normal T cells (Figure 6A and Supplemental Figure 5B), whereas DNAM1 was expressed in only 56% (13 of 23) of mPTCL cells. We detected lower expression of NKiRs, with only KLRG1, Ly49A, and Ly49G2 significantly expressed on mPTCL cells compared with normal T cells, whereas Ly49C and NKG2A were only expressed in 39% of mPTCL cells (Figure 6A and Supplemental Figure 5A). The expression of NKRs such as NKG2D or KLRG1 was associated with CD28 downregulation (Supplemental Figure 5C), confirming at the protein level that NK cell-like reprogramming of mPTCL cells was associated with the acquisition of the NKR and the loss of T cell-specific costimulatory receptors, such as CD28.

To explore whether this NK cell-like reprogramming may also take place in human PTCLs, we analyzed the expression of a set of genes associated with NK cells (e.g., NKR, NKR signaling molecules, cytotoxic molecules, etc.) in more than 250 human PTCL samples from previously published data sets (35, 36). NK/T lymphomas and HSTL originating mostly from NK cells and $\gamma\delta$ T cells, respectively, expressed most of these genes, as previously reported (Supplemental Figure 5D and refs. 35, 37). More surprisingly, this NK gene signature was also highly expressed in PTCLs originating from different entities such as ALCL-ALK⁺ and approximately half of the PTCL-NOSs analyzed. In particular, signaling molecules downstream of the NKR, such as *TYROBP*, *FCER1G*, but also *SYK* and *PLCG2*, were highly expressed in different entities such as PTCL-NOS (Supplemental Figure 5D). The heterogeneity of PTCL-NOS for the expression of this NK gene signature led us to analyze it within the 2 recently reported molecular subclassifications TBX21 and GATA3 (36). The NK gene signature was significantly enriched in PTCL-TBX21 compared with PTCL-GATA3 ($P = 0.04$, FDR = 0.09; Supplemental Figure 5, E and F), in agreement with the high T-bet expression in mPTCLs. Finally, in the TBX21 subgroup, high expression of the NK gene signature was associated with poor overall survival ($P = 0.04$; Supplemental Figure 5G).

Since we cannot rule out the possibility that some of these NK genes were expressed by the tumor microenvironment, we investigated the expression of 15 NKRs or coreceptors in 65 primary human PTCL samples representing 9 different entities using multiparametric flow cytometry, allowing gating of only lymphoma cells. The expression of NKRs and coreceptors was variable from one entity to another, with SS and T-LGL expressing most of these receptors, whereas HSTL highly expressed half of these receptors, and PTCL-NOS expressed only a few NKRs (Figure 6, B and C, and Supplemental Figure 5H). Since the anti-KIR3DL2 humanized cytotoxic antibody (lacutamab/IPH4102) showed encouraging clinical activity in a phase I trial for the treatment of CTCL (38), we focused on the expression of this KIR. Using a specific anti-KIR3DL2 antibody, we found that 9 of 14 (64%) SSs, 5 of 7 T-LGLs (71%), 5 of 19 TFH-PTCLs (26%), and 0 of 6 (0%) PTCLs-NOS were positive (Figure 6C), representing a total of 31% of the total cohort expressing KIR3DL2 (Supplemental Figure 5I). Of the 65 primary human samples tested, at least 1 KIR was expressed in 71%, at least 1 NKG2 receptor in 69%, and at least 1 natural cytotoxicity receptor (NCR) in 22% of PTCLs (Supplemental Figure 5I), demonstrating the high prevalence of NKR expression in the total human PTCL cohort.

NKaRs are functional in mPTCLs. To determine whether NKaRs expressed on mPTCLs are functional, we first confirmed the expression of Fc ϵ RI γ and DAP12 (encoded by *Tyrbp*) adaptor proteins in most mPTCLs and NK cells (Figure 7A). Stimulation of mPTCLs through NKaRs NK1.1, NKp46, and NKG2D induced significant IFN- γ expression and degranulation, as illustrated by CD107 surface expression (Figure 7B). Stimulation with plate-bound anti-CD3 led to similar results, demonstrating the cytotoxic phenotype of most mPTCLs. Triggering NKG2D, NKp46, or NK1.1 alone induced a lower but marked increase in degranulation and IFN- γ expression (Figure 7C). We observed that the effector functions of these NKaRs, alone or in combination, were completely inhibited by pretreatment with the SYK inhibitor P505-15, whereas IFN- γ and degranulation triggered by anti-CD3 were only marginally impaired, demonstrating the specific requirement for SYK in NKaR signaling but not in the TCR signaling pathway (Figure 7C). In addition, most mPTCLs expressed granzyme B, further suggesting their potential cytotoxic activity and confirming at the protein level the data from transcriptomic analyses (Figure 7D). Although some of these mPTCLs did not show any degranulation or IFN- γ expression after NKaR stimulation, these NKaRs were still functional, as evidenced by their activation of the downstream effector PLC γ 2 (Figure 7E). The activation of this effector by NKaR crosslinking was also dependent on SYK, as demonstrated by the decrease in PLC γ 2 phosphorylation in the presence of the SYK inhibitor (Figure 7E).

mPTCL survival is dependent on NKaR signaling. Given the high expression of NKaR and the constitutive activation of downstream signaling in PTCLs, we postulated that NKaR signaling could contribute to lymphoma cell survival. To test this hypothesis, mPTCL cells expressing NKG2D and NKp46 were genetically invalidated for *Klrk1* (NKG2D), *Ncr1* (NKp46), or both, to achieve a protein knockdown of NKG2D and NKp46 at rates above 90% (Supplemental Figure 6A). After transfer of the cells into syngeneic mice, we observed that the growth of mPTCLs invalidated for these

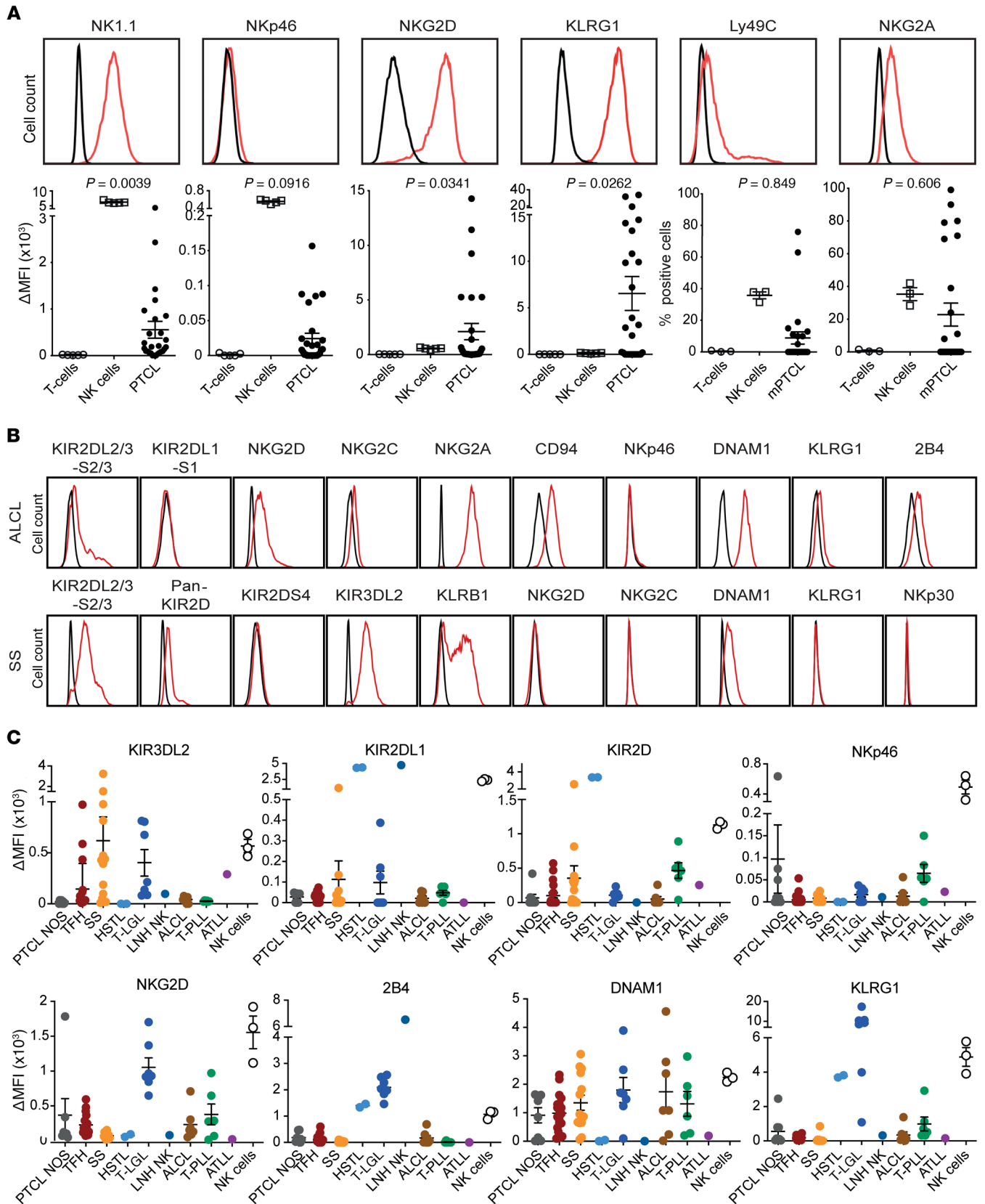


Figure 6. Murine and human PTCLs express NKR. (A) Representative histograms of NK1.1, NKp46, NKG2D, KLRG1, Ly49C, and NKG2A expression measured by flow cytometry in a single mPTCL. Associated scatter plots show expression in T cells ($n = 5$), NK cells ($n = 5$), and mPTCL cells ($n = 23$) for each NKR. P values were determined by Mann-Whitney U test comparing mPTCL cells and normal T cells. (B) Representative histograms of NKR expression in 2 human PTCLs measured by flow cytometry. (C) Scatter plot of expression of 8 different NKRs in 8 human PTCL entities established from the flow cytometric studies depicted in B. TFH-PTCL encompasses AITL and PTCL-NOS with TFH-like features according to the 2016 WHO classification. LNH NK, non-Hodgkin lymphoma from NK cells; T-PLL, T cell prolymphocytic leukemia.

genes was significantly delayed, demonstrating the contribution of NKARs to mPTCL survival in vivo (Figure 8A). From a therapeutic perspective, we also sought to determine whether pharmacological inhibition of these receptors with blocking mAbs could delay PTCL development in vivo. Such treatments were indeed sufficient to delay mPTCL development and significantly improve mouse survival compared with isotype antibody-treated control animals (Figure 8B). This effect was even stronger when we injected both anti-NKG2D- and anti-NKp46-blocking antibodies (Figure 8B), as shown by the decrease in spleen and liver volumes (Figure 8, C and D), as well as spleen and liver weights and lymphoma cell counts (Supplemental Figure 6, B and C). In addition, and consistent with the role of SYK, PLC γ 2, AKT, and S6 kinases downstream of the NKAR, treatment of mice with anti-NKG2D- and anti-NKp46-blocking antibodies reduced the constitutive activation of these kinases in mPTCL cells (Figure 8E).

We then designed a series of experiments to inhibit NKAR signaling in mPTCL in vivo. We first genetically invalidated *Syk* in mPTCL by CRISPR/Cas9, which resulted in a decrease in SYK expression (Supplemental Figure 6D) and prolonged survival of mice injected with such tumor cells as compared with the control mice (Figure 8F). We then confirmed these data using chemical inhibitors of SYK (P505-15 or cerdulatinib) or of the downstream complex mTORC1 (rapamycin) (Figure 8, G and H). To further study the role of the NKAR in mPTCL survival in vivo, we investigated the expression of the NKG2D ligands Rae and H60 in the tumor microenvironment of the spleen. We did not include the NKp46 endogenous ligand in this analysis, since this ligand remains unknown. Whereas H60 was negative in all samples tested, we found that Rae was expressed on some PTCL cells and CD31⁺ endothelial cells, as previously described (39), but was undetectable on normal T and B lymphocytes or on CD11c⁺ and CD11b⁺ cells (Supplemental Figure 6, E and F). Altogether, these results demonstrate that mPTCL cell survival is at least partially dependent on NKAR/SYK/mTOR activation through potential interaction of these receptors with their ligands expressed in the tumor microenvironment or directly on PTCL cells.

Discussion

In the present study, we developed a model in which chronic TCR stimulation was based on homeostatic proliferation that enabled polyclonal T cell activation and proliferation. Most of the mice receiving *p53*^{-/-} T cells ultimately developed PTCL, and several lines of evidence suggested a contribution of chronic

TCR engagement to these PTCLs: (a) the transfer of *p53*^{-/-} T lymphocytes in the absence of chronic TCR stimulation (*p53*KO>WT mice) did not trigger PTCL development; (b) mPTCL cells showed typical features of memory effector T cells, with some PTCL cells expressing exhaustion makers such as programmed cell death 1 (PD-1) and Lag3; (c) GSEA indicated a significant downregulation of genes in the TCR signaling pathway, as previously reported for chronically TCR-stimulated T cells (29); and (d) downregulation of CD28 and expression of NKRs on T cells have been associated with chronic TCR antigenic stimulation (40). In addition to chronic TCR stimulation, *p53* deficiency was a driver event in T cell lymphomagenesis in this model, as suggested by the absence of PTCL development in WT>CD3 ϵ ^{-/-} mice. This result is consistent with recent studies demonstrating the high prevalence of TP53 gene expression or downstream pathway alterations in several entities of human PTCL, in particular non-TFH-PTCL-NOS (4, 25), suggesting a driver role of TP53 in T cell lymphomagenesis. However, *p53* deficiency alone was not sufficient, as seen by the lack of PTCL development in the absence of chronic TCR stimulation in *p53*KO>WT mice. These data are in line with previous reports demonstrating that *p53*^{-/-} mice mainly develop immature thymic lymphomas (41, 42) and CD1d-restricted NK T cell lymphomas, but more rarely PTCLs originating from conventional T cells (23, 24).

Most PTCLs generated in our study model exhibited a NK-like phenotype consistent with a reprogramming that was probably the consequence of chronic TCR stimulation. Indeed, NKR⁺ T cells, in particular NKR⁺ CD8⁺ T cells, have been associated with antigen-experienced T cells during chronic infection (40, 43) and in autoimmune disorders such as systemic lupus erythematosus (SLE) (44), rheumatoid arthritis (45), and celiac disease (46). In addition to chronic TCR stimulation, IL-15 was recently described as a key driver in this reprogramming during acute hepatitis A infection, in which memory CD8⁺ T cells expressed NKG2D and NKp30 (47), and in patients with SLE with NKp30-expressing CD8⁺ T cells (44). In the mPTCL model presented here, the maintenance of CD122 expression, even though CD25 was downregulated, was consistent with a joint role of chronic TCR stimulation and IL-15 in the NK-like reprogramming. In normal thymocytes and mature CD8⁺ T cells, reprogramming toward NK-like cells has been described upon *Bcl11b* deletion (33). These reprogrammed NK-like cells are fully functional, since they can kill tumor cells in vitro and prevent tumor metastasis in vivo (33). In our model, further study will be necessary to ascertain whether *Bcl11b* downregulation is first triggered by chronic TCR stimulation that consequently leads to NK-like reprogramming.

NKRs, in particular NKARs, appeared to be markers of general NK-like reprogramming. The results of our study emphasized their functional role in PTCL in major cellular pathways, such as those for cytotoxicity, proliferation, and/or survival. So, NKAR genetic invalidation or blocking antibodies targeting NKp46 and NKG2D significantly delayed PTCL development in vivo, highlighting the importance of these NKARs in PTCL survival (Figure 8, A and B). Involvement of NKARs in normal NK and T cell survival and proliferation was formerly established in particular with NKG2C, Ly49D, and DNAM1 (46, 48–53). In addition, engagement of CD16 strongly supports leukemia

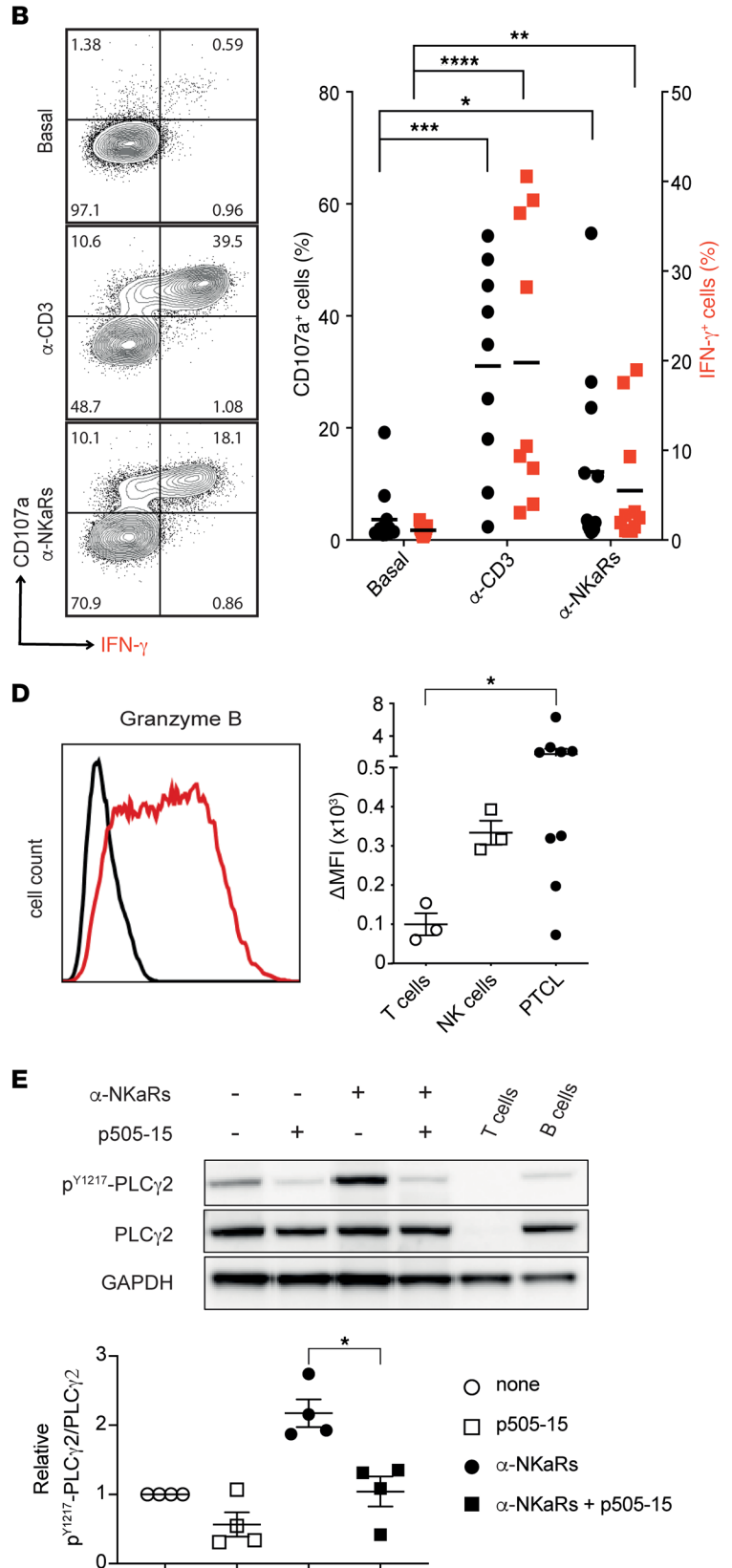
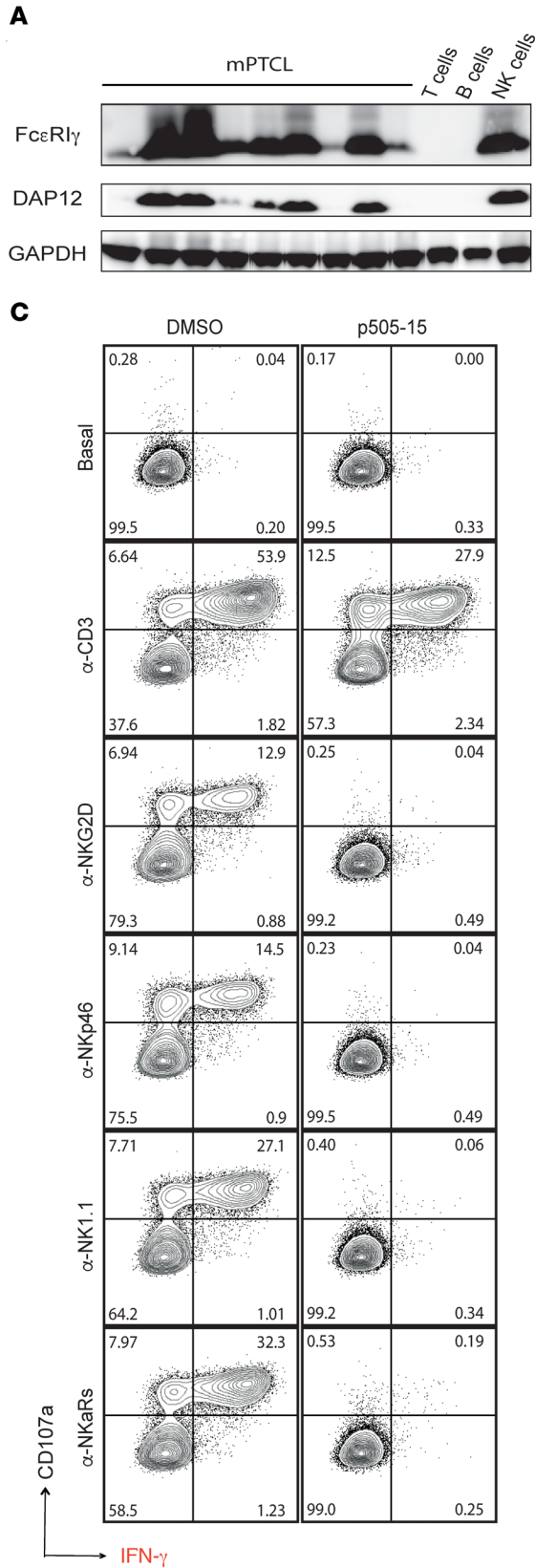


Figure 7. NKR are functional and signal through SYK in mPTCLs. (A) Western blots showing expression of the adaptor proteins FcεR1g and DAP12 in 9 mPTCL samples. Enriched NK cells and sorted B and T cells were used as positive and negative controls, respectively. GAPDH was used as a loading control. **(B)** Representative FACS analysis of CD107a and IFN- γ expression in a cytotoxicity assay of mPTCL cells in the basal state and after NKaR or TCR-CD3 complex activation. Scatter plot shows CD107a (black) and IFN- γ (red) expression in the basal state ($n = 12$), after anti-CD3/anti-CD28 ($n = 9$, PTCL cells expressing low levels of CD3 were not analyzed) and after NKR activation ($n = 12$) (right panel). $*P < 0.05$, $**P < 0.01$, $***P < 0.001$, and $****P < 0.0001$, by Mann-Whitney U test with Holm's post hoc correction. **(C)** Representative FACS analysis of CD107a and IFN- γ expression in mPTCL cells in the basal state or activated with anti-CD3/CD28 (α -CD3) or anti-NKaR (α -NKaRs) in the presence of vehicle or P505-15. Data are representative of 2 different mPTCLs. **(D)** Representative FACS analysis of granzyme B expression in mPTCL cells (red) compared with staining with an isotype control (black). Scatter plot shows granzyme B expression in normal T cells ($n = 3$), NK cells ($n = 3$), and mPTCL cells ($n = 9$). $*P < 0.05$, by Mann-Whitney U test comparing mPTCL cells and normal T cells. **(E)** Western blots show p^{Y127}-PLC γ 2 and total PLC γ 2 expression in a representative mPTCL in the basal state and after NKaR in vitro activation in the presence of vehicle or P505-15. The relative phosphorylation of p^{Y127}-PLC γ 2/total PLC γ 2 of 4 mPTCLs was quantified in these different conditions. Sorted stimulated B and T cells from WT mice were used as positive and negative controls, respectively. GAPDH was used as a loading control. $*P < 0.05$, by Mann-Whitney U test.

cell proliferation in T-LGL (54, 55), and KIR3DL2 regulates cell survival of Sézary cells by inhibiting apoptosis induced by TCR stimulation (56).

In humans, we identified several PTCL entities, such as T-LGL and SS, that expressed most of the NKRs tested in our study. The role of chronic TCR stimulation in these entities has been proposed (19, 20), however, whether NKR expression is triggered by chronic TCR stimulation or other chronic inflammatory signals such as IL-15, which has undoubtedly been associated with lymphomagenesis of these 2 entities (31, 32), is still a matter of debate. NKaR expression has been described in several other human PTCL entities and is often considered a hallmark of the innate-like T cell origin of these PTCLs (57–59). Indeed, a NK-like cytotoxic signature has been described in MEITL that may be associated with the $\gamma\delta$ T cell origin of these lymphoma cells (59). However, whole-exome sequencing revealed that 30% of MEITLs had *BCL11B* mutations (59), suggesting that reprogramming may also explain this NK-like signature. Results from our mouse model may also lead to a reconsideration of the cell of origin of these PTCLs as the only explanation for this NK cell-like phenotype, since we demonstrated that chronically stimulated conventional T cells reprogram into innate-like T cells expressing NKaRs.

Our analysis of transcriptomic data revealed that approximately 50% of PTCL-NOSs exhibited a NK gene signature that was mostly associated with the PTCL-TBX21 subgroup and a poor clinical outcome for patients, in line with previous reports (36). We also unraveled the expression of several NKRs on ALK⁻ and ALK⁺ ALCL cells, as already partially described in previous studies (60). SYK and PLC γ 2 are also expressed in a significant proportion of ALCLs, especially in ALK⁺ cases, corroborating previous data reporting SYK expression in CD30⁺ PTCL (61) and SYK-dependent growth and survival of ALK⁺ PTCL cell lines (62). In the case of ALK⁺ ALCL, nucleophosmin-ALK (NPM-ALK) fusion protein

activates various signaling pathways, such as PI3K/AKT/mTOR, RAS/ERK, and PLC γ (63–65), mimicking chronic TCR signaling that could lead to NKR and SYK expression. Expression of the NKR and SYK in ALK⁻ ALCL could also be due to chronic TCR stimulation. This was recently suggested in breast implant-associated ALK⁻ ALCL, in which downregulation of TCR signaling genes was evidenced by GSEA (21). Interestingly, a profound downmodulation of *BCL11b* expression has been associated with *BCL11B* promoter methylation in ALCL (66), suggesting that NK-like reprogramming of ALCL could also be driven by the loss of *BCL11b* expression. Whether this is also the consequence of chronic TCR stimulation requires further experiments. Thus, the expression of SYK and NKRs by ALCL cells could result from lymphomagenesis steps similar to those observed in our mouse model, especially since this entity shows recurrent p53 pathway alterations (67).

In conclusion, our results provide evidence that chronic TCR stimulation triggers PTCL development. This chronic TCR stimulation promotes epigenetic T cell reprogramming toward NK-like cells, downregulating several T cell-specific genes, such as *Bcl11b* and inducing several NK cell features, such as NKRs and their signaling molecules. We also demonstrated that this NK-like reprogramming induced addiction to SYK and NKaR signaling to maintain PTCL survival, whereas TCR signaling was mostly ineffective. Thus, we found that TCR signaling, despite being required for lymphomagenesis, does not constitute an optimal target in established PTCL, as previously reported in AITL (13). Our investigations led us to propose that NKR and SYK expression in several human PTCL entities emerging from conventional T cells could result from chronic TCR stimulation and epigenetic NK-like reprogramming. We believe our study has important clinical implications and highlights the potential interest of immunotherapies targeting the NKR in human PTCLs. One direct outcome of this work may be to foster the use of the anti-KIR3DL2 humanized cytotoxic antibody lcutamab (IPH4102), not only to treat CTCLs but also to treat KIR3DL2⁺ PTCLs, which represent more than 30% of the cohort tested in our human study. In addition to the TELLO-MAK clinical trial (NCT03902184), a new multi-cohort phase II trial focused on anti-KIR in T cell lymphoma (KILT) is currently underway to assess the impact of lcutamab in combination with gemcitabine and oxaliplatin (GEMOX) in such PTCLs at relapse. In addition to previous reports (62, 68), our study also reveals the clinical translational finding that some PTCLs show constitutive expression and activation of SYK, raising the possibility of testing new SYK inhibitors in patients with PTCL, as illustrated by the encouraging results from a phase II trial of cerdulatinib (NCT04021082) that demonstrated responses in 35% of patients with PTCL and in 35% of those with CTCL (69).

Methods

See Supplemental Methods for further details.

Data availability. Microarray data from mPTCLs and normal control T cells have been deposited in the NCBI's Gene Expression Omnibus (GEO) database (GEO GSE174257) Microarray data from Immunological Genome Project (ImmGen) murine populations (www.ImmGen.org) were collected from the ImmGen database (accession number GPL6246). ATAC-Seq data from mPTCLs and normal control T cells, as well as from NKT cells and NK cells have been deposited in

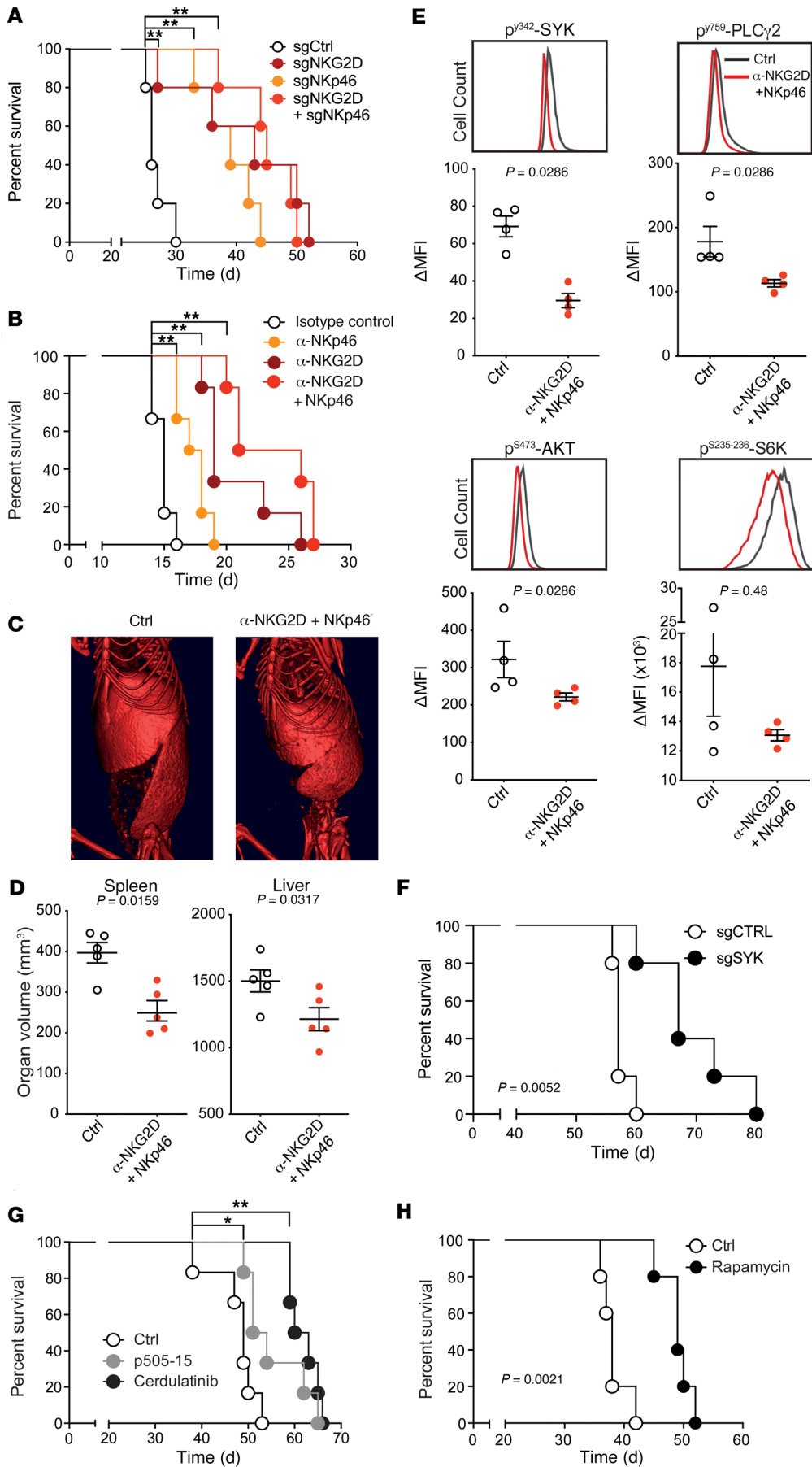


Figure 8. mPTCL cells rely on NKαR signaling for survival. (A) Kaplan-Meier survival curves for WT mice ($n = 5$ for each group) transferred with mPTCL cells genetically invalidated for *Klrk1* (sgNKG2D), *Ncr1* (sgNKp46), or both, using Alt-R CRISPR/Cas9 sgRNA targeting these genes, or transfected with control sgRNA. $**P < 0.01$, by log-rank test with Holm's post hoc correction. Data are representative of 2 independent experiments using different mPTCL cells. (B) Kaplan-Meier survival curves for mPTCL-bearing NSG mice treated with isotype control or anti-NKp46- and anti-NKG2D-blocking mAbs alone or in combination ($n = 6$ for each group). $**P < 0.01$, by log-rank test with Holm's post hoc correction. Data are representative of 3 independent experiments using different PTCLs. (C) Representative 3D reconstruction of spleen and liver of mPTCL-bearing NSG mice treated with isotype control or a combination of anti-NKp46- and anti-NKG2D-blocking mAbs and sacrificed 12 days after PTCL transfer for analysis. (D) Spleen and liver volumes of mPTCL-bearing NSG mice treated with a combination of anti-NKp46- and anti-NKG2D-blocking mAbs or isotype control 12 days after PTCL transfer (isotype control group, $n = 5$; mAb-treated group, $n = 5$). P values were determined by Mann-Whitney U test. (E) FACS analysis of p-SYK, p-PLCγ2, p-AKT, and p-S6 and associated scatter plots of mPTCL cells from PTCL-bearing mice treated with anti-NKG2D- and anti-NKp46-blocking mAbs ($n = 4$) or isotype control ($n = 4$). (F) Kaplan-Meier survival curves for WT mice ($n = 5$ for each group) transferred with mPTCL cells genetically invalidated for *Syk* (sgSYK) or transfected with control sgRNA. P value was determined by log-rank test. Data are representative of 2 independent experiments using different mPTCLs. (G) Kaplan-Meier survival curves for mPTCL-bearing NSG mice treated with vehicle alone (Ctrl) or with either P505-15 (20 mg/kg) or cerdulatinib (20 mg/kg). $*P < 0.05$ and $**P < 0.01$, by log-rank test with Holm's post hoc correction. Data are representative of 2 independent experiments using different PTCLs. (H) Kaplan-Meier survival curves for mPTCL-bearing NSG mice treated with vehicle control or rapamycin. P value was determined by log-rank test. Data are representative of 2 independent experiments using different PTCLs.

the GEO database (GEO GSE174576). ATAC-Seq data from ImmGen murine populations were collected from the ImmGen database (accession number SRP110978).

Statistics. Statistical analyses were conducted using Microsoft Excel 2013 and GraphPad Prism, version 6.0 (GraphPad Software). Results are reported as the mean \pm SD unless otherwise stated. We performed analyses of significance using the Mann-Whitney U or Kruskal-Wallis test. Continuous biological variables were assumed to follow a normal distribution. A P value of less than 0.05 was considered statistically significant. Survival in mouse experiments is represented as a Kaplan-Meier curve, and the log-rank test was used to determine the significance. All of the experiments were repeated at least twice, and representative images are shown.

Study approval. All animal studies and procedures were performed in accordance with European Union guidelines and approved by the local Animal Ethics Evaluation Committee (CECCAPP, SFR Biosciences, Gerland, France, UMS3444/US8). Human samples used for flow cytometric analysis were obtained from frozen cell suspension collections from the Centre de Ressources Biologiques of the Centre Hospitalier Lyon Sud and the Centre Hospitalier Universitaire Grenoble Alpes and from the CeVi collection of the Institut Carnot/CALYM (ANR, France; <https://www.calym.org/-Viable-cell-collection-CeVi-.html>).

For histopathology and IHC, paraffin-embedded samples were obtained from tissue collections of the Centre Hospitalier Lyon Sud

(CHLS) and the TENOMIC consortium. For all human samples, the patients provided written informed consent.

The clinical outcomes of the patients with PTCL-NOS described in Supplemental Figure 5 were previously reported (36).

Author contributions

SC, DC, and MH performed in vivo and in vitro experiments and data analysis and designed and interpreted the study. AM, MU, and RR performed in vivo and in vitro experiments and data analysis. AC, AV, E. Bardel, CF, LC, and C. Lours performed in vivo and in vitro experiments and data analysis. SM, AB, RMP, AF, EJ, and SS performed bioinformatics analysis. JPR, JI, PS, and TW performed data analysis and reviewed the manuscript. C. Lefebvre, DS, LDL, PG, MB, GS, and E. Bachy provided patient samples, performed data analysis, and reviewed the manuscript. CB and ATG performed and analyzed the immunohistochemical studies. SC and LG wrote the manuscript and prepared the figures. E. Bachy and LG conceived and designed the study. LG supervised, analyzed, and interpreted the study.

Acknowledgments

We thank N. Aguilera, J.F. Henry, P. Manas (PBES, SFR Biosciences Gerland, UMS3444/US8) for their help at the animal care facility; T. Andrieu and S. Dussergey (SFR Biosciences Gerland, UMS3444/US8) for technical assistance with cell sorting; Simon de Bernard and Laurent Buffat (Altrabio) for assistance with the GEP analysis; and M. Billaud and B. Manship for critical reading of the manuscript. We are indebted to the NIH Tetramer Core Facility for providing the mouse CD1d tetramers. The authors would like to thank the LYSA-Pathology and the Plateforme de Ressources Biologiques at Henri Mondor Hospital for technical assistance and the participants of the TENOMIC Consortium (see Supplemental Acknowledgments for details on the TENOMIC Consortium). Frozen primary human PTCLs were obtained through the CeVi_Collection Project from the Institut Carnot CALYM funded by the French National Research Council (Agence Nationale de la Recherche [ANR]) (<https://experts-recherche-lymphome.org/>) and the Centers for Biological Resources of Lyon (BRIF: BB-0033-00046) and Grenoble (BRIF: BB-0033-00069). E. Bachy was funded by the European Union Transcan-2 "ERANET-PLL" grant. LG was supported by INSERM, The Institut Carnot CALYM, La Ligue Nationale Contre le Cancer (LNCC) – Equipe Labellisée LIGUE 2017, and INCa-DGOS-INSERM_12563 for the LYriCAN project. SC was supported by a Fondation pour la Recherche Médicale (FRM) fellowship.

Address correspondence to: Laurent Genestier, Université Claude Bernard Lyon I, Faculté de Médecine Lyon sud, 165 Chemin du Petit Revoyet, 69921 Oullins Cedex, France. Phone: 33.0.4.26.23.59.81; Email: laurent.genestier@inserm.fr. SC's present address is: Department of Genetic of Hematological Malignancies, Grenoble University Hospital, Grenoble, France. GS's present address is: Lymphoma Service, Memorial Sloan Kettering Cancer Center, New York, USA.

1. Swerdlow SH, et al. The 2016 revision of the World Health Organization classification of lymphoid neoplasms. *Blood*.

2016;127(20):2375–2390.

2. Fiore D, et al. Peripheral T cell lymphomas: from the bench to the clinic. *Nat Rev Cancer*.

2020;20(6):323–342.

3. Pechloff K, et al. The fusion kinase ITK-SYK mimics a T cell receptor signal and drives

- oncogenesis in conditional mouse models of peripheral T cell lymphoma. *J Exp Med.* 2010;207(5):1031-1044.
4. Choi J, et al. Genomic landscape of cutaneous T cell lymphoma. *Nat Genet.* 2015;47(9):1011-1019.
 5. Ungewickell A, et al. Genomic analysis of mycosis fungoides and Sézary syndrome identifies recurrent alterations in TNFR2. *Nat Genet.* 2015;47(9):1056-1060.
 6. da Silva Almeida AC, et al. The mutational landscape of cutaneous T cell lymphoma and Sezary syndrome. *Nat Genet.* 2015;47(12):1465-1470.
 7. Kataoka K, et al. Integrated molecular analysis of adult T cell leukemia/lymphoma. *Nat Genet.* 2015;47(11):1304-1315.
 8. Palomero T, et al. Recurrent mutations in epigenetic regulators, RHOA and FYN kinase in peripheral T cell lymphomas. *Nat Genet.* 2014;46(2):166-170.
 9. Yoo HY, et al. A recurrent inactivating mutation in RHOA GTPase in angioimmunoblastic T cell lymphoma. *Nat Genet.* 2014;46(4):371-375.
 10. Sakata-Yanagimoto M, et al. Somatic RHOA mutation in angioimmunoblastic T cell lymphoma. *Nat Genet.* 2014;46(2):171-175.
 11. Vallois D, et al. Activating mutations in genes related to TCR signaling in angioimmunoblastic and other follicular helper T cell-derived lymphomas. *Blood.* 2016;128(11):1490-1502.
 12. Abate F, et al. Activating mutations and translocations in the guanine exchange factor VAV1 in peripheral T cell lymphomas. *Proc Natl Acad Sci U S A.* 2017;114(4):764-769.
 13. Cortes JR, et al. RHOA G17V Induces T follicular helper cell specification and promotes lymphomagenesis. *Cancer Cell.* 2018;33(2):259-273.
 14. Ng SY, et al. RhoA G17V is sufficient to induce autoimmunity and promotes T cell lymphomagenesis in mice. *Blood.* 2018;132(9):935-947.
 15. Warner K, et al. T cell receptor signaling in peripheral T cell lymphoma - a review of patterns of alterations in a central growth regulatory pathway. *Curr Hematol Malig Rep.* 2013;8(3):163-172.
 16. Murray A, et al. Study of the immunohistochemistry and T cell clonality of enteropathy-associated T cell lymphoma. *Am J Pathol.* 1995;146(2):509-519.
 17. Ritter J, et al. T cell repertoires in refractory celiac disease. *Gut.* 2018;67(4):644-653.
 18. Belhadji K, et al. Hepatosplenic gammadelta T cell lymphoma is a rare clinicopathologic entity with poor outcome: report on a series of 21 patients. *Blood.* 2003;102(13):4261-4269.
 19. Garrido P, et al. Monoclonal TCR-Vbeta13.1+/CD4+/NKa+/CD8-/dim T-LGL lymphocytosis: evidence for an antigen-driven chronic T cell stimulation origin. *Blood.* 2007;109(11):4890-4898.
 20. Tothova SM, et al. Mycosis fungoides: is it a *Borrelia burgdorferi*-associated disease? *Br J Cancer.* 2006;94(6):879-883.
 21. Di Napoli A, et al. Transcriptional analysis distinguishes breast implant-associated anaplastic large cell lymphoma from other peripheral T cell lymphomas. *Mod Pathol.* 2019;32(2):216-230.
 22. Wang X, et al. TCR-dependent transformation of mature memory phenotype T cells in mice. *J Clin Invest.* 2011;121(10):3834-3845.
 23. Bachy E, et al. CD1d-restricted peripheral T cell lymphoma in mice and humans. *J Exp Med.* 2016;213(5):841-857.
 24. Robinot R, et al. Chronic *Borrelia burgdorferi* infection triggers NKT lymphomagenesis. *Blood.* 2018;132(25):2691-2695.
 25. Watatani Y, et al. Molecular heterogeneity in peripheral T cell lymphoma, not otherwise specified revealed by comprehensive genetic profiling. *Leukemia.* 2019;33(12):2867-2883.
 26. Crescenzo R, et al. Convergent mutations and kinase fusions lead to oncogenic STAT3 activation in anaplastic large cell lymphoma. *Cancer Cell.* 2015;27(4):516-532.
 27. Jiang L, et al. Exome sequencing identifies somatic mutations of DDX3X in natural killer/T cell lymphoma. *Nat Genet.* 2015;47(9):1061-1066.
 28. Surh CD, Sprent J. Homeostasis of naive and memory T cells. *Immunity.* 2008;29(6):848-862.
 29. Baniyash M. TCR zeta-chain downregulation: curtailing an excessive inflammatory immune response. *Nat Rev Immunol.* 2004;4(9):675-687.
 30. Sato N, et al. Development of an IL-15-autocrine CD8 T cell leukemia in IL-15-transgenic mice requires the cis expression of IL-15R. *Blood.* 2011;117(15):4032-4040.
 31. Mishra A, et al. Aberrant overexpression of IL-15 initiates large granular lymphocyte leukemia through chromosomal instability and DNA hypermethylation. *Cancer Cell.* 2012;22(5):645-655.
 32. Mishra A, et al. Mechanism, consequences, and therapeutic targeting of abnormal IL15 signaling in cutaneous T cell lymphoma. *Cancer Discov.* 2016;6(9):986-1005.
 33. Li P, et al. Reprogramming of T cells to natural killer-like cells upon Bcl11b deletion. *Science.* 2010;329(5987):85-89.
 34. Daussy C, et al. T-bet and Eomes instruct the development of two distinct natural killer cell lineages in the liver and in the bone marrow. *J Exp Med.* 2014;211(3):563-577.
 35. Travert M, et al. Molecular features of hepatosplenic T cell lymphoma unravels potential novel therapeutic targets. *Blood.* 2012;119(24):5795-5806.
 36. Iqbal J, et al. Gene expression signatures delineate biological and prognostic subgroups in peripheral T cell lymphoma. *Blood.* 2014;123(19):2915-2923.
 37. Lima M. Extranodal NK/T cell lymphoma and aggressive NK cell leukaemia: evidence for their origin on CD56+bright CD16-/dim NK cells. *Pathology.* 2015;47(6):503-514.
 38. Bagot M, et al. IPH4102, a first-in-class anti-KIR3DL2 monoclonal antibody, in patients with relapsed or refractory cutaneous T cell lymphoma: an international, first-in-human, open-label, phase 1 trial. *Lancet Oncol.* 2019;20(8):1160-1170.
 39. Thompson TW, et al. Endothelial cells express NKG2D ligands and desensitize antitumor NK responses. *Elife.* 2017;6:e30881.
 40. Seyda M, et al. T cells going innate. *Trends Immunol.* 2016;37(8):546-556.
 41. Donehower LA, et al. Mice deficient for p53 are developmentally normal but susceptible to spontaneous tumours. *Nature.* 1992;356(6366):215-221.
 42. Jacks T, et al. Tumor spectrum analysis in p53-mutant mice. *Curr Biol.* 1994;4(1):1-7.
 43. Seich Al Basatena NK, et al. KIR2DL2 enhances protective and detrimental HLA class I-mediated immunity in chronic viral infection. *PLoS Pathog.* 2011;7(10):e1002270.
 44. Correia MP, et al. Distinct human circulating NKp30⁺FcεRIγ⁺CD8⁺ T cell population exhibiting high natural killer-like antitumor potential. *Proc Natl Acad Sci U S A.* 2018;115(26):E5980-E5989.
 45. Yen JH, et al. Major histocompatibility complex class I-recognizing receptors are disease risk genes in rheumatoid arthritis. *J Exp Med.* 2001;193(10):1159-1167.
 46. Meresse B, et al. Reprogramming of CTLs into natural killer-like cells in celiac disease. *J Exp Med.* 2006;203(5):1343-1355.
 47. Kim J, et al. Innate-like cytotoxic function of bystander-activated CD8⁺ T cells is associated with liver injury in acute hepatitis A. *Immunity.* 2018;48(1):161-173.
 48. Smith HR, et al. Recognition of a virus-encoded ligand by a natural killer cell activation receptor. *Proc Natl Acad Sci U S A.* 2002;99(13):8826-8831.
 49. Brown MG, et al. Vital involvement of a natural killer cell activation receptor in resistance to viral infection. *Science.* 2001;292(5518):934-937.
 50. Daniels KA, et al. Murine cytomegalovirus is regulated by a discrete subset of natural killer cells reactive with monoclonal antibody to Ly49H. *J Exp Med.* 2001;194(1):29-44.
 51. Dokun AO, et al. Specific and nonspecific NK cell activation during virus infection. *Nat Immunol.* 2001;2(10):951-956.
 52. Lopez-Verges S, et al. Expansion of a unique CD57(+)NKG2Chi natural killer cell subset during acute human cytomegalovirus infection. *Proc Natl Acad Sci U S A.* 2011;108(36):14725-14732.
 53. Nabekura T, et al. Costimulatory molecule DNAM-1 is essential for optimal differentiation of memory natural killer cells during mouse cytomegalovirus infection. *Immunity.* 2014;40(2):225-234.
 54. Hoshino S, et al. Activation via the CD3 and CD16 pathway mediates interleukin-2-dependent autocrine proliferation of granular lymphocytes in patients with granular lymphocyte proliferative disorders. *Blood.* 1991;78(12):3232-3240.
 55. Cambiaggi A, et al. The natural killer-related receptor for HLA-C expressed on T cells from CD3+ lymphoproliferative disease of granular lymphocytes displays either inhibitory or stimulatory function. *Blood.* 1996;87(6):2369-2375.
 56. Ghazi B, et al. KIR3DL2/CpG ODN interaction mediates Sézary syndrome malignant T cell apoptosis. *J Invest Dermatol.* 2015;135(1):229-237.
 57. Uemura Y, et al. Expression of activating natural killer-cell receptors is a hallmark of the innate-like T cell neoplasm in peripheral T cell lymphomas. *Cancer Sci.* 2018;109(4):1254-1262.
 58. Ettersperger J, et al. Interleukin-15-dependent T cell-like innate intraepithelial lymphocytes develop in the intestine and transform into lymphomas in celiac disease. *Immunity.* 2016;45(3):610-625.
 59. Moffitt AB, et al. Enteropathy-associated T cell lymphoma subtypes are characterized

- by loss of function of SETD2. *J Exp Med*. 2017;214(5):1371–1386.
60. Freud AG, et al. Expression of the activating receptor, Nkp46 (CD335), in human natural killer and T cell neoplasia. *Am J Clin Pathol*. 2013;140(6):853–866.
61. Bisig B, et al. CD30-positive peripheral T cell lymphomas share molecular and phenotypic features. *Haematologica*. 2013;98(8):1250–1258.
62. Wilcox RA, et al. Inhibition of Syk protein tyrosine kinase induces apoptosis and blocks proliferation in T cell non-Hodgkin's lymphoma cell lines. *Leukemia*. 2010;24(1):229–232.
63. Slupianek A, et al. Role of phosphatidylinositol 3-kinase-Akt pathway in nucleophosmin/anaplastic lymphoma kinase-mediated lymphomagenesis. *Cancer Res*. 2001;61(5):2194–2199.
64. Bai RY, et al. Nucleophosmin-anaplastic lymphoma kinase of large-cell anaplastic lymphoma is a constitutively active tyrosine kinase that utilizes phospholipase C-gamma to mediate its mitogenicity. *Mol Cell Biol*. 1998;18(12):6951–6961.
65. Amin HM, Lai R. Pathobiology of ALK+ anaplastic large-cell lymphoma. *Blood*. 2007;110(7):2259–2267.
66. Hassler MR, et al. Insights into the pathogenesis of anaplastic large-cell lymphoma through genome-wide DNA methylation profiling. *Cell Rep*. 2016;17(2):596–608.
67. Parrilla Castellar ER, et al. ALK-negative anaplastic large cell lymphoma is a genetically heterogeneous disease with widely disparate clinical outcomes. *Blood*. 2014;124(9):1473–80.
68. Feldman AL, et al. Overexpression of Syk tyrosine kinase in peripheral T cell lymphomas. *Leukemia*. 2008;22(6):1139–1143.
69. Horwitz SM, et al. A phase 2 study of the dual SYK/JAK inhibitor cerdulatinib demonstrates good tolerability and clinical response in relapsed/refractory peripheral T-cell lymphoma and cutaneous T-cell lymphoma. *Blood*. 2019;134(Suppl 1):466.